Available online at www.sciencedirect.com
ScienceDirect
Journal of Computational Physics 224 (2007) 403–413
JOURNAL OF COMPUTATIONAL PHYSICS
www.elsevier.com/locate/jcp

Numerical zoom for multiscale problems with an application to nuclear waste disposal

Jean-Baptiste Apoung Kamga [a], Olivier Pironneau [b,*]

[a] *Laboratoire Jacques-Louis Lions and IUF, Université Pierre et Marie Curie, Place Jussieu, 75005 Paris, France*
[b] *Université Pierre et Marie Curie and IUF, France*

Received 3 October 2006; received in revised form 19 March 2007; accepted 22 March 2007
Available online 5 April 2007

Abstract

We analyse here a computational technique and error estimates for the numerical solution of some problems with multiple scales when the small scale is confined to geometrically small regions such as jumps of coefficients on curves and surfaces or complex variations of coefficients in small regions where numerical zooms can be made. The method is an adaptation of the Hilbert Subspace Decomposition Method studied by the second author in a different context so the method is restated with all known results. Combined with the layer decomposition of [S. Delpino, O. Pironneau, Asymptotic analysis and layer decomposition for the Couplex exercise, in: Alain Bourgeat, Michel Kern (Eds.), Computational Geosciences, vol. 8. No. 2, Kluwer Academics Publishers, 2004, pp. 149–162] the method is applied to the numerical assessment of a nuclear waste repository site.
© 2007 Elsevier Inc. All rights reserved.

PACS: 02.30.Jr; 47.11.Fg; 28.41.Kw; 47.55.P–

Keywords: Multiscale; Finite element; Domain decomposition; Chimera; Numerical zoom; Nuclear waste

1. Introduction

The present paper deals with the numerical difficulties found in connection with multiscales when they are geometrically confined in a small region of the computational domain while an accurate answer requires a computation in the entire domain. The analysis is applied to a geophysical problem in the context of nuclear waste disposal, but similar situations are encountered often in other fields.

Steger [15,16] introduced his Chimera method in a similar context to compute the flow around a wing-engine configuration; ever since composite grids have been very popular in CFD (see for example [11]). The motivation was different however because finite difference methods could not handle such a complex

* Corresponding author. Tel.: +33 1 44 27 44 11; fax: +33 1 44 27 72 00.
E-mail addresses: apoung@ann.jussieu.fr (J.-B. Apoung Kamga), Olivier.Pironneau@upmc.fr (O. Pironneau).

0021-9991/$ - see front matter © 2007 Elsevier Inc. All rights reserved.
doi:10.1016/j.jcp.2007.03.020

geometry while it could be used on the wing or the engine alone. Nevertheless the basic idea of seeing the flow around the engine as a correction to the one around the wing has been a seminal one. It is even more spectacular when applied to cases where one geometrical domain is much larger than the other as for the computation of a the drag of a rivet on a wing. In such case every engineer computes the wing first and then zoom in the rivet and recompute the flow locally with the main flow as boundary condition. But what do we know about the numerical error involved in such decomposition? For nuclear waste this is an important question because the repository sites must be validated to be legal.

It is easy to see that Chimera is a domain decomposition method as introduced by Schwarz in the late 19th century. Conceptually the computational domain Ω is decomposed into two or more overlapping domains, $\Omega = \Omega_1 \cup \Omega_2$; two new boundaries appear, $\Gamma_{ij} = \partial\Omega_i \cap \Omega_j$, $i, j = 1, 2, i \neq j$ and the so-called Schwarz multiplicative algorithm with overlapping subdomains is

(1) Choose $\phi_i^0, i = 1, 2$.
(2) Compute ϕ_i^{m+1} by solving the problem in Ω_i with $\phi_i^{m+1} = \phi_j^m$ on Γ_{ij}.
(3) Iterate until convergence.

Convergence has been established by Lions [12] in the continuous case when the decomposition is non-degenerated, i.e. when Ω_i is not strictly inside Ω_j in the discrete case it is still an open problem when the meshes do not share common nodes and edges.With non-overlaping meshes the problem has been solved by Hansbo et al. [10] and certainly one could also try to apply a zoom strategy in their context of non-overlaping Schwarz algorithm.

In the wing-rivet problem more than one iteration is almost never done. In Steger's case however one iteration was not enough and so air outside the wing could not be the computational domain; an area smaller than the engine had to be dug out to avoid degeneracy, but as it could be aligned with the mesh the meshing problem was easy.

In [13] Lions and Pironneau proposed a similar decomposition with the idea in mind that a domain built by Constructive Solid Geometry, as in some CAD systems, could offer a numerical advantage for PDEs. The idea was to attach to each subdomain Ω_i its own contribution ψ_i to the full solution ψ. In a variational context a PDE is set in a Hilbert space V, $H_0^1(\Omega)$ for instance, and so the method was to write

$$\psi = \sum_i \psi_i, \quad \psi_i \in V_i \tag{1}$$

where V_i is a subspace of V attached to the subdomain Ω_i, such as $H_0^1(\Omega_i)$. So the method was conveniently called HSDM, short for Hilbert Subspace Decomposition Method. In the case of Laplace's equation with homogeneous Dirichlet boundary data and a source term f, it amounts to find $\{\psi_i\}_1^I$ such that $\psi_i \in H_0^1(\Omega_i)$ and

$$\int_{\Omega_i} \left(\nabla \sum_j \psi_j \right) \nabla w = \int_{\Omega_i} fw \quad \forall w \in H_0^1(\Omega_i) \ \ \forall i \tag{2}$$

There is no hope to find a unique solution because the decomposition (1) is usually not unique, so a stabilization term is added in the iterative process:

- Choose $\psi_i^0, i = 1..I$ and $\beta > 0$.
- For each i solve

$$\int_{\Omega_i} \left(\beta(\psi_i^{m+1} - \psi_i^m) w + \nabla \psi_i^{m+1} \nabla w + \nabla \left(\sum_{j \neq i} \psi_j^m \right) \nabla w \right) = \int_{\Omega_i} fw \quad \forall w \in H_0^1(\Omega_i) \tag{3}$$

- Iterate in m until convergence.

At the continuous level the method turns out to be nothing else than Steger's Chimera when $I = 2$, $V_i = H_0^1(\Omega_i)$ and the Ω_i make an overlapping non-degenerate decomposition of Ω; this is seen with

$\phi_i^{m+1} = \psi_i^{m+1} + \psi_i^m$. However, here there is a major gain in that the decomposition can be degenerate and yet convergence holds. So true zooming is possible with Ω_2 a subset of Ω_1 and ψ_2 a correction to ψ_1.

Concurrently Glowinski, He and Rappaz introduced in [8] a similar method, with the idea that if a problem has multiple scales it might be possible to attach a correction ϕ_i to each scale. For example, knowing that $f = f_0 + \delta_z$ where f_0 is smooth and δ_z is a Dirac mass at $z \in \Omega$ on can solve (2) with f_0 attached to ψ_1 and then add the solution of the same with $f = \delta_z$ which is then attached to ψ_2. After formalization the method comes to be almost the same as HSDM but in their second paper [9] (see also [18]) a very useful estimate is obtained for the discretization of (2) on independent meshes of size H for Ω_1 and h for Ω_2:

$$\|\phi_H^1 + \phi_h^2 - \phi\|_1 \leqslant C\left(H^r \|\phi\|_{H^{r+1}_{\Omega_1}} + h^s \|\phi\|_{H^{s+1}_{\Omega_2}}\right) \tag{4}$$

where r and s are the degree of the finite element method to compute ϕ_H^1 and ϕ_h^2.

The discretization of (3) by the finite element method converges with the estimate (4) but it involves a complex integral of product of functions defined on different meshes; it can be computed exactly if the meshes are intersected, an operation which is easy in 2D and almost impossible in 3D, at least with tetraedra. Quadrature errors can deteriorate the method but a workable quadrature was obtained in [6,4], furthermore, in the discrete case $\beta = 0$ is admissible because the solution is usually unique (see below).

The paper has two parts, one in which the method is presented with all the results mentioned above and the other were it is applied to the difficult problem of nuclear waste repository assessment.

2. Nuclear waste repository assessment exercises

The French government has decided to build a laboratory to test the feasibility of a repository site south of Nancy, east of Paris, for nuclear waste. The site must be assessed numerically and safety must be demonstrated for a few hundred thousand years; as there are numerous uncertainties in the geological parameters it is important to be sure of the numerical scheme and its precision.

ANDRA posted in 2000 a numerical challenge to assess the efficiency of numerical methods and softwares for their problems, together with a test case called Couplex [1,3]. In 2006, a second test case was posted [17] with a more realistic 3D geometry.

The challenge is an idealized vault which lies 450 m deep inside a clay layer, which has above it a layer of limestone and a layer of marl, and below it a layer of dogger-limestone.

Water flows slowly through these porous media in a saturated state and convects the radioactive materials after some thousands of years when the canisters have rusted.

The first problem then is to compute accurately the hydrostatic pressure by Darcy's law. For stationary flow in a saturated medium this is a simple elliptic partial differential equation with non-constant coefficients, but the difficulty lies in the very large variation of these coefficients from one layer to the next. The coefficient κ which appears in the Darcy operator $\nabla \cdot (\kappa \nabla \phi)$ for the hydrostatic pressure ϕ is in principle a tensor, but for simplicity here it is taken diagonal and isotropic in each layer: The enormous difference of values could yield a precision problem but by a simple argument of domain decomposition we can split sequentially the problem into four subproblems, one in each layer, as explained in [7]. The method is briefly restated in Paragraph 2.2 below with a new proof of convergence; it implies that a geological layer sandwiched between two layers with much smaller permeability can be computed independently with homogeneous Neumann conditions on the boundary.

Still the aspect ratio of the clay layer which contains the repository is also enormous as it is some 10 km long and only 450 m high. It is there that a zooming strategy is required and the core of the paper is about the precision of such a strategy.

Finally, for the convection diffusion of the radionucleides , the source is localized in a very small region and the zoom strategy will rely on this property.

These two techniques have allowed us to do on a standard PC simulations which would have required parallel computing.

3. Layer decomposition

3.1. Solution over the whole domain

Except for the top layer which does not cover the whole ground surface, the computational domain is cylindrical with horizontal scales greater than 10 km and depth only a few hundred meters, but the layers are almost horizontal and the interfaces between layers are plane as a first approximation. Darcy's law in a saturated medium gives the velocity of the water $u = -\kappa\nabla\phi$ in terms of the hydrostatic pressure ϕ and incompressibility, namely $\nabla \cdot u = 0$, gives an equation for ϕ, which when completed with appropriate boundary conditions is written as

$$\nabla \cdot (\kappa\nabla\phi) = 0 \quad \text{in } \Omega, \quad \phi|_{\partial\Omega_d} = \phi_\Gamma, \quad \kappa\nabla\phi \cdot n|_{\partial\Omega_n} = g \tag{5}$$

where the boundary of the domain has a Dirichlet part $\Gamma_d := \partial\Omega_d$ and a Neumann part $\Gamma_n := \partial\Omega_n$ and where n is the outer normal to the Neumann part.

A direct approximation of the full problem has been done with linear finite elements on a tetrahedral mesh but the usual error estimates give no information on the precision obtained because of the huge difference of κ in each layer. Indeed the standard error estimates for (5) discretized by the finite element method of degree 1 on triangles/tetraedra of size h is at best:

$$\|\nabla\phi_h - \nabla\phi\| < C\sqrt{\frac{\kappa_{\max}}{\kappa_{\min}}}h$$

Fig. 1 displays the results;the color ranges from 180 to 420.

3.2. Domain decomposition

Consider a domain Ω made of two layers $\Omega_i, i = 0, 1$ with Darcy coefficient κ_i in Ω_i and $\Gamma_{01} = \bar{\Omega}_0 \cap \bar{\Omega}_1$ the interface boundary.

Denote by $\phi|_i$ the restriction to Ω_i of the solution of (5). If there is sufficient regularity two compatibility conditions hold at the interface:

$$\phi|_0 = \phi|_1, \qquad \kappa_0 \frac{\partial\phi|_0}{\partial n_0} = -\kappa_1 \frac{\partial\phi|_1}{\partial n_1} \quad \text{on } \Gamma_{01}$$

Therefore, if $\kappa_0 \gg \kappa_1$ and is constant in Ω_i then the problem decouples and can be solved in sequence:

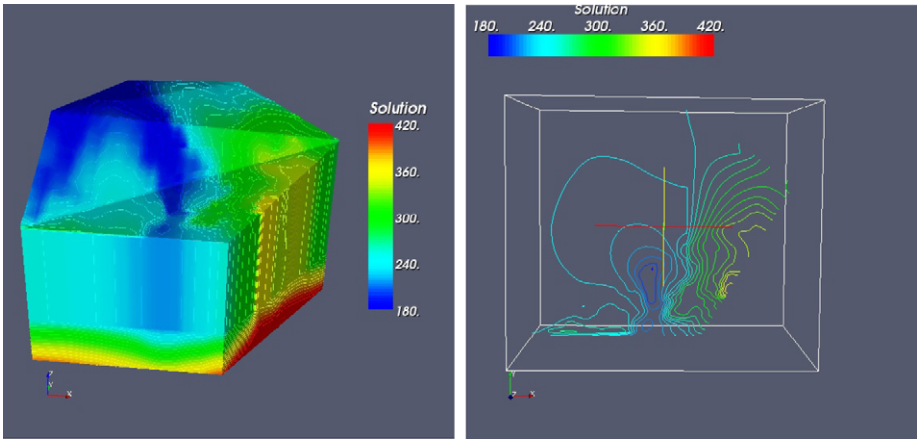

Fig. 1. Solution of the full problem with a finite element of degree 1 on triangles.

$$\begin{aligned} &\text{Step 1}: \Delta\phi_0 = 0 \quad \text{in } \Omega_0, \quad \frac{\partial\phi_0}{\partial n}|_{\Gamma_{01}} = 0 \\ &\text{Step 2}: \Delta\phi_1 = 0 \quad \text{in } \Omega_1, \quad \phi_1|_{\Gamma_{01}} = \phi_0 \end{aligned} \tag{6}$$

plus the condition on $\partial\Omega$. The error made is as follows.

Proposition 1. *Let ϕ_c be ϕ_i in $\Omega_i, i = 1, 2$ solution of (6). Let ϕ be the solution of (5); then*

$$\|\phi_c - \phi\|_{1,\Omega} \leqslant C\frac{\kappa_1}{\kappa_0}(\|g\|_{-\frac{1}{2},\Gamma_n} + \|\phi_\Gamma\|_{\frac{1}{2},\Gamma_d}) \tag{7}$$

Proof. For simplicity we assume that the support of g is in $\Gamma_n \cap \partial\Omega_0$; the results holds also in the general case but the notations are more complex and g should be replaced by κg. Let $\varepsilon = \kappa_1/\kappa_0$ and $\phi = \phi^0 + \varepsilon\phi^1 + \varepsilon^2\phi^2_\varepsilon$, the solution of problem (5):

$$\int_\Omega (I_{\Omega_0} + \varepsilon I_{\Omega_1})\nabla(\phi^0 + \varepsilon\phi^1 + \varepsilon^2\phi^2_\varepsilon)\cdot\nabla w = \frac{1}{\kappa_0}\int_{\Gamma_n} gw \tag{8}$$

Let us choose $\phi^0|_{\Omega_0} = \phi_0$ and $\phi^0|_{\Omega_1} = \phi_1$ defined in (6) and ϕ^1 such that

$$\int_{\Omega_0} \nabla\phi^1\cdot\nabla w + \int_{\Omega_1}\nabla\phi^0\cdot\nabla w = 0$$

and such that $\Delta\phi^1 = 0$ in Ω_1 and ϕ^1 continuous on Γ_{01}. Then (8) implies

$$\int_\Omega \kappa\nabla\phi^2_\varepsilon\cdot\nabla w + \int_{\Omega_1}\nabla\phi^1\cdot\nabla w = 0 \tag{9}$$

All above holds for any $w \in V$, the subset of $H^1_0(\Omega)$ of functions with zero trace on Γ_d.

By this construction ϕ^1 is bounded by ϕ^0 and so ϕ^2_ε is bounded at worse by $\varepsilon^{-1}\phi^1$. Therefore

$$\|\phi - \phi^0\| = \varepsilon\|\phi^1 + \varepsilon\phi^2_\varepsilon\| \leqslant C\varepsilon\|\phi^0\|$$

But ϕ^0 is ϕ_c and it is bounded by the data g and ϕ_Γ.

3.3. Application

Let us apply this to the Couplex problem. We define three independent parameters $\varepsilon_1, \varepsilon_2, \varepsilon_3$ which are the ratios between the coefficients κ in each zones:

$$\varepsilon_1 = \frac{\kappa_{\text{Kim-cov}}}{\kappa_{\text{Kim-not-cov}}} = \frac{1}{3}10^{-7}, \quad \varepsilon_2 = \frac{\kappa_{\text{Kim-cov}}}{\kappa_{\text{Oxf}}} = \frac{1}{2}10^{-4}, \quad \varepsilon_3 = \frac{\kappa_{\text{Cal-Oxf}}}{\kappa_{\text{Oxf}}} = 10^{-4}$$

According to Proposition 1, we will have a precision 10^{-4} if we solve the problem in cascade:

- *Step 1*: Solve (5) first in the Tithonian + Kimmeridian with homogeneous Neumann conditions at the interface with other layers and the given conditions elsewhere.
- *Step 2*: Solve (5) in the Kimmeridian covered layer with Dirichlet conditions $\phi = \phi_i$, obtained from step 1 with homogeneous Neumann conditions on unspecified boundaries.

The advantage is that now each problem has constant coefficients and the operator becomes the Laplace operator.

We have a similar decomposition below with the Oxfordian computed first.

We have applied this decomposition with P^1 tetraedric meshes in each layer. Results are shown in Fig. 2 and compared with the global solution of the previous section. The overall precision is better than ε_3. The gain

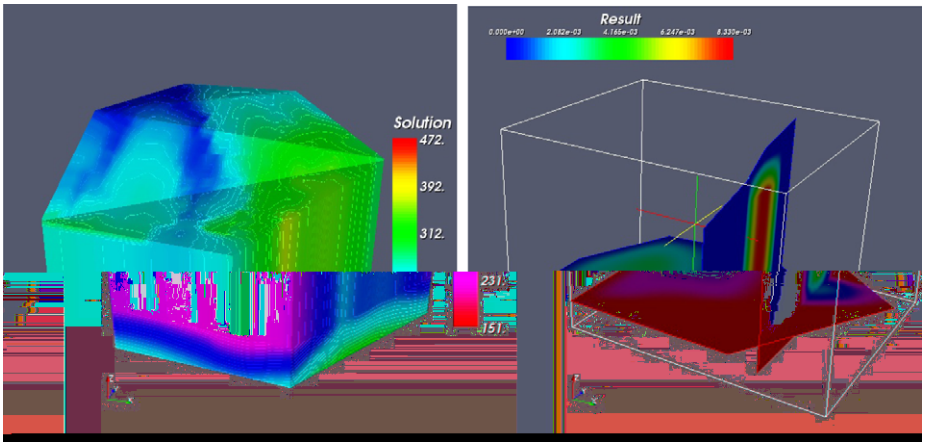

Fig. 2. Solution within each layer (left, the color range is (151,472)) and difference between the global computation and the computation layer by layer (right, the color range is (0,8.33e−3)).

in CPU is of course enormous because the full linear system which was solved with the conjugate Gradient method and a tridiagonal preconditioner has been broken into several smaller and better conditioned linear systems small enough to be solved by a multifrontal direct method such as UMFPACK (in www.cise.ufl.edu/research/sparse/umfpack/).

4. Numerical zoom near the repository

The repository is made of numerous galleries which are reinforced with concrete and filled with containers and swelling clay; each region has its own Darcy coefficient κ but also around some galleries there may be a fractured zone due to the drilling, and we wish to study the effect on the flow of such a zone modelled by a Darcy constant hundred times larger than in the unfractured medium. The geometry of the galleries is so complex that a mesh capable of representing it would be much too fine except may be for the largest supercomputers; in particular the mesh used above cannot represent such a geometry.

4.1. A finite element zoom

So let us use (2) with $\Omega_1 = \Omega$ the whole clay layer and Ω_2 a close up, preferably convex, simply connected region containing all the galleries but not much more.

Let V_H and V_h^2 be piecewise linear continuous triangular finite element discretizations of $V = \{v \in H_0^1(\Omega) : v|_{\Gamma_d} = 0\}$ and $H_0^1(\Omega_2)$, respectively. Subscript H indicates that we use a coarse triangulation $\mathcal{T}_H$ for Ω and h indicates a fine triangulation $\mathcal{T}_h$ of max size h for Ω_2.

We solve the following problem: given an interpolation $\phi_{\Gamma H}$ of the Dirichlet boundary conditions, find $\phi_H^1 - \phi_{\Gamma H} \in V_H$ and $\phi_h^2 \in V_h^2$ such that

$$\int_\Omega (\kappa \nabla(\phi_H^1 + \phi_h^2)\nabla(w_H^1 + w_h^2)) = \int_{\Gamma_n} g(w_H^1 + w_h^2) \quad \forall w_H^1 \in V_H,\ \ w_h^2 \in V_h^2 \tag{10}$$

Existence and uniqueness was proved in [6] and as said earlier the proof of (4) is in [8] but an extension to three meshes is given in Appendix A.

Remark 1. In $\Omega \setminus \Omega_2$ the hydrostatic pressure ϕ is smooth while $\|\phi\|_{2,\Omega_2}$ grows with the ratio of κ in the clay and in the galleries. So h/H should be chosen accordingly.

4.2. Implementation

The following iterative process can be used:

$$\begin{aligned}\int_\Omega \left(\beta(\phi_H^{1^{m+1}} - \phi_H^{1^m})w_H^1 + \kappa\nabla(\phi_H^{1^{m+1}} + \phi_h^{2^m})\nabla w_H^1\right) &= \int_{\Gamma_n} g w_H^1 \quad \forall w_H^1 \in V_H \\ \int_\Omega \left(\beta(\phi_h^{2^{m+1}} - \phi_2^{2^m})w_h^2 + \kappa\nabla(\phi_H^{1^m} + \phi_h^{2^{m+1}})\nabla w_h^2\right) &= 0 \quad \forall w_h^2 \in V_h^2\end{aligned} \tag{11}$$

The integrals of $\kappa\nabla\phi_H^1 \cdot \nabla w_h^2$ and of $\kappa\nabla\phi_h^2 \cdot \nabla w_H^1$ cannot be computed exactly except by intersecting the two meshes $\mathscr{T}_H$ and $\mathscr{T}_h$. The following quadrature formula was proposed in [6] for the integral of $\nabla u \cdot \nabla v$ over $\Omega_1 \cup \Omega_2$:

$$a_h(u,v) = \sum_{k=1}^{N_H} \sum_{j=1..3} \frac{|T_k^1|}{3} \kappa \frac{\nabla u \cdot \nabla v}{I_{\Omega^1} + I_{\Omega^2}}\bigg|_{\xi_{jk}^1} + \sum_{k=1}^{N_h} \sum_{j=1..3} \frac{|T_k^1|}{3} \kappa \frac{\nabla u \cdot \nabla v}{I_{\Omega^1} + I_{\Omega^2}}\bigg|_{\xi_{jk}^2} \tag{12}$$

where N_H, N_h are the number of triangles and where the gradients are computed on their native triangulations and evaluated at the quadrature points ξ; for each triangle of both triangulations 3ξ are chosen, one near each vertex. In (12), I_Ω denotes the indicator function of Ω.

In [6] it was also shown that the bilinear form in (12) is strongly elliptic. The continuity of the elliptic form requires another hypothesis:

Proposition 2. *If in addition no quadrature point of $\mathscr{T}_h$ are on an edge (resp face in 3D) of $\mathscr{T}_H$ and conversely then the bilinear form in (12) is continuous and coercive so that problem (5) with (12) is well posed and the quadrature formula does not degrade the error estimate (4).*

The proof can be found in [4]. This was done in the context of domain decomposition, however, it is clearly not optimal in the context of patches because we want a quadrature formula of precision $O(h)$ in the patch. It seems that one can use a Gauss quadrature on the vertices of the patch only; the error analysis is still in progress.

4.3. Zoom as corrector

One nice property of the above zoom procedure is that ϕ_H^1 is an $O(1)$ H-approximation of the solution and ϕ_h^2 is an $O(H+h)$ correction, driving the error to $O(h)$.

Proposition 3.

$$\|\phi_h^2\|_{1,\Omega_2} \leqslant C(H+h)$$

The proof is a straightforward application of the triangular inequality to (4):

$$\|\phi_h^2\| \leqslant \|\phi_h^2 + \phi_H^1 - \phi\| + \|\phi_H^1 - \phi\| \tag{13}$$

The first term on the right is $O(H+h)$ while the second is $O(H)$.

4.4. Recursive zoom

Now suppose that a second correction $\phi_\hbar^3$ is computed by solving over a smaller domain $\Omega_3 \subset \Omega_2$ triangulated by $\mathscr{T}_\hbar$ with $\hbar \ll h$:

$$\int_\Omega (\kappa\nabla(\phi_H^1 + \phi_h^2 + \phi_\hbar^3)\nabla(w_H^1 + w_h^2 + w_\hbar^3)) = \int_{\Gamma_n} g(w_H^1 + w_h^2 + w_\hbar^3) \quad \forall w_H^1 \in V_H,\ w_h^2 \in V_h^2,\ w_\hbar^3 \in V_\hbar^3 \tag{14}$$

If H and h are chosen so that $\|\phi_H^1 + \phi_h^2 - \phi\|$ is $O(\varepsilon)$, and $\hbar$ is chosen so that $\|\phi_H^1 + \phi_h^2 + \phi_\hbar^3 - \phi\|$ is $O(\varepsilon')$ with $\varepsilon' \ll \varepsilon$ then, using (4) extended to three meshes (see Appendix A)

$$\|\phi_\hbar^3\| \leqslant \|\phi_\hbar^3 + \phi_h^2 + \phi_H^1 - \phi\| + \|\phi_h^2 + \phi_H^1 - \phi\| \leqslant C(\varepsilon + \varepsilon') \tag{15}$$

In the case of the vault and its galleries, the second zoom leaves out some galleries in which $\|\phi\|_{2,\mathrm{loc}}$ is not small; for instance, h can be adhoc to describe the galleries but not the fractured zone around some galleries. Suppose we are interested by a region in which $\hbar$ is fine enough to describe all the details, fractured zone, canisters, etc. of one gallery; suppose the numerical zoom is only in this gallery and not elsewhere, then by making use of the following estimate we can assess the error made.

Proposition 4. *Let ϕ and ψ be the solutions of*

$$\begin{aligned} &-\nabla\cdot(\kappa_0\nabla\phi) = f \quad \text{in } \Omega, \phi|_{\partial\Omega} = \phi_\Gamma \\ &-\nabla\cdot(\kappa\nabla\psi) = f \quad \text{in } \Omega, \psi|_{\partial\Omega} = \phi_\Gamma \end{aligned} \tag{16}$$

where $\kappa = \kappa_0$ except inside a connected region D of boundary Σ strictly inside Ω where $\kappa = \kappa_1$. Assume that κ_0, κ_1 are smooth everywhere and constant in D and $f|_D = 0$, then the following holds:

$$|\phi-\psi|(x) \leqslant C\frac{|\kappa_1-\kappa_0|}{d(x,\Sigma)}(\|f\|_0 + \|\phi_\Gamma\|_{1/2,\Gamma}) \quad \forall x \notin D \tag{17}$$

for some C depending on κ and Σ, where d denotes the distance of x to Σ.

The proof rely on the fact that the Green function $G(x,y)$ of the first problem

$$-\nabla\cdot(\kappa_0\nabla G)(y) = \delta_x(y), \;\; y\in\Omega, \quad G|_{\partial\Omega} = 0$$

decays like $|x-y|^{-1}$. Indeed, let $\xi = \phi - \psi$

$$\begin{aligned} \xi(x) &= \int_{\Omega\setminus\Sigma}\delta_x(y)\xi(y) = -\int_{\Omega\setminus\Sigma}\nabla\cdot(\kappa_0\nabla G(x,y))\xi(y) \\ &= -\int_{\Omega\setminus\Sigma}\nabla\cdot(\kappa_0\nabla\xi(y))G(x,y) + \int_\Sigma \kappa_0\left(\frac{\partial G}{\partial n}[\phi] - \left[\frac{\partial\xi}{\partial n}\right]G\right) = \int_\Sigma \kappa_0\left[\frac{\partial\psi}{\partial n}\right]G(x,y)\mathrm{d}y \end{aligned} \tag{18}$$

Now $|[\partial_n\psi]| = |\frac{[\kappa]}{\kappa_1}\partial_n\psi|$, $\|\partial_n\psi\|_{-1/2,\Sigma}$ is bounded by $C(|f|_0 + \|\phi_\Gamma\|_{1/2})$ and $\|G(x,.)\|_{\infty,\Sigma}$ is bounded by a $C/d(x,\Sigma)$ for some C (see [14]).

Remark 2. when several regions Σ_i have $\kappa \neq \kappa_0$ the estimate contains $d(x,\Sigma_i)^{-1}$ so in the example of Fig. 2 the zoom is outside all the blind galleries containing the other canisters but their distance to the zoom region makes their influence small. The main gallery is more problematic because the part just outside the zoom is not correctly meshed if it is not homogeneous. Thus at the level of the first zoom the mesh should be refined near to the second zoom.

Fig. 3 shows the results of a local computation around all galleries (first zoom) in the clay layer, followed by a zoom around one of the blind gallery containing the canisters (second zoom). The second geometry accounts for the fractured zone, the cement of the gallery and the swelling clay around the canisters in the center of the gallery for the values of the parameters, see Table 1.

After the second zoom the first one is recomputed but the changes are hardly visible (see Table 2); a more detailed report on numerical convergence for a simpler 2D test case can also be found in [2,4].

5. Convection–diffusion of radionucleides

After a few thousands of years some canister leak. The radionucleides are dissolved in the ambiant water and the concentration of each element, like iodine I^{129}, $c(x,t)$, is given by

$$\begin{aligned} &\alpha\frac{\partial c}{\partial t} + \beta c + u\cdot\nabla c - \nabla\cdot(v\nabla c) = 0 \quad \text{in } \Omega\times(0,T) \\ &c(\cdot,0) = c^0 \quad \text{in } \Omega, \qquad c \text{ or } \frac{\partial c}{\partial n} = 0 \quad \text{on } \partial\Omega \end{aligned} \tag{19}$$

where α accounts for the sorption in the medium, β accounts for the radioactivity decay, $u = -\kappa\nabla\phi$ is the convection by the Darcy flow and v is the diffusion tensor of the medium.

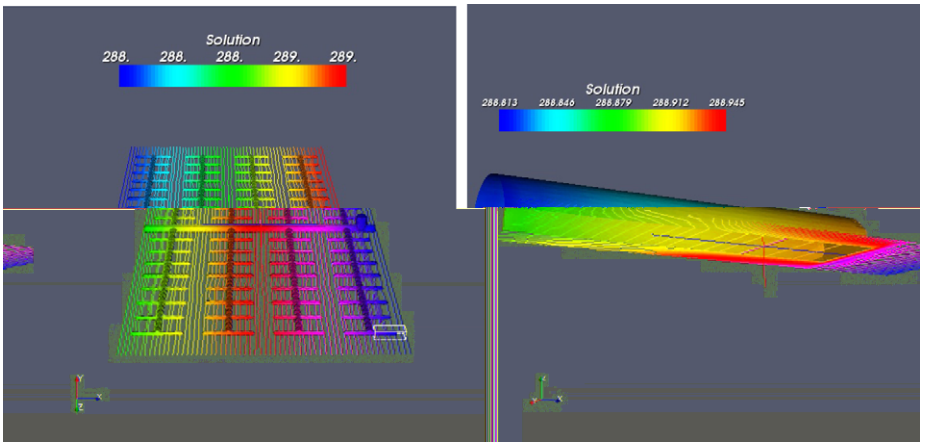

Fig. 3. Hydrostatic pressure near the galleries: Second and third zoom from data computed by layer decomposition. The second iteration with results of the first on the finest zoom (right, the color range is (288, 289)) did not alter in any visible way the results on the left. The picture on the right displays the level lines (the range is (288.813, 288.945)) on an horizontal cross section through the symmetry plane of the gallery and a color map of the hydrostatic pressure on the surface of the part of the gallery above the cross section.

Table 1
Permeability coefficient in each layer

Hydrogeologic layers	Permeability K (m/s)	
	Regional	Local
Tithonian	3×10^{-5}	3×10^{-5}
Kimmeridgian not covered	3×10^{-4}	3×10^{-4}
Kimmeridgian covered	10^{-11}	10^{-12}
Oxfordian L2a–L2b	2×10^{-7}	10^{-9}
Oxfordian Hp1–Hp4	6×10^{-7}	8×10^{-9}
Oxfordian C3a–C3b	10^{-10}	10^{-12}
Callovo-Oxfordien (Cox)	$K_v = 10^{-14}, K_h = 10^{-12}$	

Table 2
Convergence history between the first and the second zoom for two different values of the porosity of the concrete κ_c the L^∞ and L^2 norms are shown for $u^{m+1} - u^m$

m	$\frac{\kappa_c}{\kappa_{clay}}$	$\|u_H^{m+1} - u_H^m\|_\infty$	$\|u_h^{m+1} - u_h^m\|_\infty$	$\|u_H^{m+1} - u_H^m\|_0$	$\|u_h^{m+1} - u_h^m\|_0$
0	10^{-1}	6.49×10^{-4}	0.017	4.88×10^{-6}	0.07
1	10^{-1}	1.55×10^{-5}	1.96×10^{-4}	5.64×10^{-7}	6.30×10^{-7}
0	10^{-5}	2.59×10^{-4}	0.043	1.25×10^{-6}	0.228
1	10^{-5}	1.46×10^{-5}	1.14×10^{-4}	5.65×10^{-7}	6.76×10^{-7}

The source term is an initial condition because the time over which a canister leaks is short in geological terms. So c^0 is confine geometrically to a very small region of space within the gallery where the second zoom is made.

If G is the Green function of problem (19) then

$$c(x,t) = \int_\Omega G(x-y,t)c^0(y)\mathrm{d}y \tag{20}$$

By a change of variable (19) rewritten in a Lagrangian frame is similar but with $u = 0$ and a classical estimate (see [5] for example) tells us that there exists C such that

$$|G(x-y,t)| \leqslant \frac{C}{t^{3/2}}\mathrm{e}^{-\frac{|x-y|^2}{Ct}} \tag{21}$$

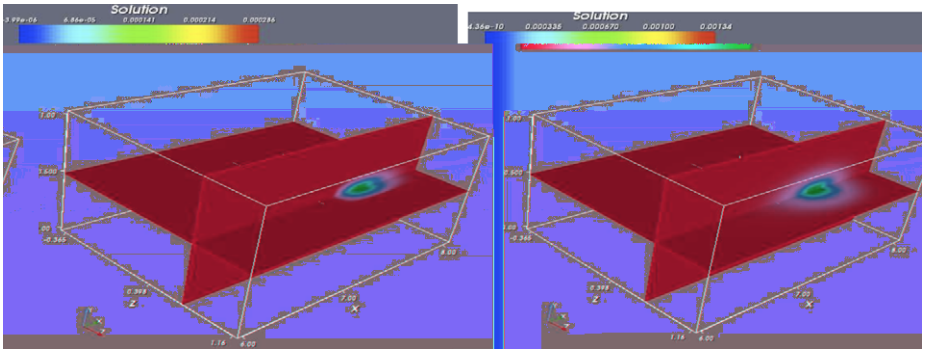

Fig. 4. Concentration of iodine due to the break up of a canister in a gallery.On the left the color spectrum is $(-3.99\text{e}{-6}, 0.000286)$ and on the right $(4.36\text{e}{-10}, 0.00134)$.

Therefore, coming back to the physical domain

$$c(x,t) < |D||c^0|_\infty \frac{C}{t^{3/2}} \mathrm{e}^{-\frac{|x-x_D|^2}{Ct}-\beta t} \tag{22}$$

where D is the support of c^0 augmented by a region of diameter $|u|_{\max} t/\alpha$ and x_D is the point in D closest to x.

This gives us the tool to limit the computational domain, at least for a short geological time.

Proposition 5. *Let c be the solution of (19) and $\tilde{c}$ the solution of the same but in $\widetilde{\Omega}$ containing D. Then*

$$\|\tilde{c} - c\| \leqslant C_1 |c^0|_\infty \frac{C}{t^{3/2}} \mathrm{e}^{-\frac{|x-x_D|^2}{Ct}-\beta t} \tag{23}$$

This inequality holds because both c and $\tilde{c}$ are solutions of the same equation on $\widetilde{\Omega}$ but with different Dirichlet boundary conditions; so (23) is a consequence of the continuity of the solution with respect to boundary data.

Remark 3. In practice it is better to compute $\tilde{c}$ with Neumann conditions on $\widetilde{\Omega}$ because one can then check the size of c on $\partial\Omega$ and stop the computation when it is too large. After that time $\tilde{t}$ a bigger computational domain can be chosen and the simulation is reinitialized with $c^0 = \tilde{c}(\cdot, \tilde{t})$. Then the mesh can be coarse because $\tilde{c}$ is spread over a large domain.

In Fig. 4 a simulation of the early stage of break up of the canister is done, first near the canister itself then in a bigger domain

6. Conclusion

We have presented and analysed a numerical zoom strategy in the elliptic case. We have shown that the method is feasible and adapted to cases where the complexity of the solution is only in a small part of the geometry. With the Hilbert Subspace Decomposition Method, iterations should be performed between the zoom region and the full domain, however, the size of the irregularities both in number and in geometrical size greatly reduce the number of iterations and indeed in several case it is possible to use one iteration only as done in practice in engineering but this is not justified by the error analysis. Such methods, combined here with other multiscale techniques like the layer decomposition here make it possible to compute on desktop machines what normally would require a supercomputer.

Appendix A. Extension of (4) to three meshes

This proof is a straightforward adaptation of the one given in [18]

Let u be solution of a strongly elliptic bilinear variational problem

$$a(u,v) = (f,v) \quad \forall v \in H_0^1(\Omega); \quad u \in H_0^1(\Omega) \tag{A.1}$$

Let $u_{Hh\hbar}$ denote a function which is the sum of a function of $V_H \subset H_0^1(\Omega)$ plus a function of $V_h \subset H_0^1(D)$ plus a function of $V_\hbar \subset H_0^1(O)$ where these are finite element spaces of degree one over triangulations of Ω, $D \subset \Omega$ and $O \subset D$, respectively. Let $u_{Hh\hbar} \in V_H + V_h + V_\hbar$ be a solution of

$$a(u_{Hh\hbar}, v_{Hh\hbar}) = (f, v_{Hh\hbar}) \quad \forall v_{Hh\hbar} \in V_H + V_h + V_\hbar \tag{A.2}$$

For some $u^1 \in H_0^1(\Omega)$, $u^2 \in H_0^1(D)$, $u^3 \in H_0^1(O)$, we choose $w_H = \pi_H u^1$, $w_h = \pi_h u^2$, $w_\hbar = \pi_\hbar u^3$, where the π are the interpolants on the meshes. Let $w_{Hh\hbar} = w_H + w_h + w_\hbar$ and $v_{Hh\hbar} = u_{Hh\hbar} - w_{Hh\hbar}$. The following holds:

$$a(u, v_{Hh\hbar}) = a(u_{Hh\hbar}, v_{Hh\hbar}) \quad \text{and so } a(v_{Hh\hbar}, v_{Hh\hbar}) = a(u - w_{Hh\hbar}, v_{Hh\hbar})$$

Therefore, $\|v_{Hh\hbar}\| \leqslant \|u - w_{Hh\hbar}\|$ and so

$$\|u - u_{Hh\hbar}\| \leqslant \|u - w_{Hh\hbar}\| + \|v_{Hh\hbar}\| \leqslant 2\|u - w_{Hh\hbar}\|$$

Finally, if $u^1 + u^2 + u^3 = u$,

$$\|u - w_{Hh\hbar}\| \leqslant \|u^1 - w_H\| + \|u^2 - w_h\| + \|u^3 - w_\hbar\| \leqslant C(H\|u^1\|_2 + h\|u^2\|_2 + \hbar\|u^3\|_2) \tag{A.3}$$

Now it remains to choose the u^i intelligently.

By taking u^1 to be an extension in D of $u|_{\Omega\setminus D}$ we secure $\|u^1\|_2 \leqslant \|u\|_{2,\Omega\setminus D}$ and we notice that $v^1 := u - u^1 \in H_0^1(D)$ and $\|v^1\|_2 = \|u - u^1\|_{2,D}$.

Next, by taking u^2 to be an extension in O of $v^1|_{\Omega\setminus O}$ we secure $u^2 - v^1 \in H_0^1(O)$ and $\|u^2\|_2 = \|v^1\|_{2,D\setminus O}$.

Now $u^3 := u - u^1 - u^2 = v^1 - u^2 \in H_0^1(O)$ and so $\|u^3\|_2 = \|u^3\|_{2,O}$.

This proves that

$$\|u - u_{Hh\hbar}\| \leqslant C(H\|u\|_{2,\Omega\setminus D} + h\|u\|_{2,D\setminus O} + \hbar\|u\|_{2,O}) \tag{A.4}$$

References

[1] ANDRA, Couplex test cases, 2001. <http://www.andra.fr/couplex>.

[2] J.B. Apoung-Kamga, Eléments finis discontinus et zoom numérique. Thèse, université Paris VI, December 2006. <www.ann.jussieu.fr/pironneau/theseJBApoung.pdf>.

[3] A. Bourgeat, M. Kern, S. Scumacker, J. Talandier, The Couplex test cases: nuclear waste disposal simulation, Comput. Geosci. 8 (2004) 83–87.

[4] J.B. Apoung-Kamga, O. Pironneau, A numerical quadrature for the Schwarz–Chimera method, in: D. Keyes (Ed.), Proceedings of the Domain Decomposition Conference, New York, January 2005.

[5] D.G. Aronson, Bounds for the fundamental solution of a parabolic equation, Bull. AMS 73 (1967) 890–896.

[6] F. Brezzi, J.L. Lions, O. Pironneau, Analysis of a Chimera method, CRAS 332 (2001) 655–660.

[7] S. Delpino, O. Pironneau, Asymptotic analysis and layer decomposition for the Couplex exercise, in: Alain Bourgeat, Michel Kern (Eds.), Computational Geosciences, vol. 8. No. 2, Kluwer Academics Publishers, 2004, pp. 149–162.

[8] R. Glowinski, J. He, J. Rappaz, J. Wagner, Approximation of multi-scale elliptic problems using patches of finite elements, C. R. Acad. Sci. Paris, Ser. I 337 (2003) 679–684.

[9] R. Glowinski, J. He, A. Lozinski, J. Rappaz, J. Wagner, Finite element approximation of multi-scale elliptic problems using patches of elements, Numer. Math. 101 (4) (2005) 663–687.

[10] A. Hansbo, P. Hansbo, M.G. Larson, A finite element method on composite grids based on Nitche's method, ESAIM: M2AN 37 (2003) 495–514.

[11] W.D. Henshaw, On multigrid for overlapping grids, William D. Henshaw, SIAM J. Sci. Comput. 26 (2005) 1547–1572.

[12] P.L. Lions, On the Schwarz alternating method, I, II, III, in: Symposium on Domain Decomposition Methods for Partial Differential Equations, SIAM series, Philadelphia, 1988, pp. 89–90.

[13] J.L. Lions, O. Pironneau, Algorithmes parallèles pour la solution de problèmes aux limites, CRAS 327 (1998) 947–952.

[14] W. Littman, G. Stampaccia, H. Weinberger, Regular point for elliptic equations with discontinuous coefficients, Ann. Sc. Norm. Sup. Pisa 17 (1963) 45–79.

[15] J.L. Steger, J.A. Benek, On the use of composite grid schemes in computational aerodynamics, Comput. Methods Appl. Mech. Eng. 64 (1987) 301–320.

[16] J.L. Steger, The Chimera method of flow simulation, in: Workshop on Applied CFD, University of Tennessee Space Institute, 1991.

[17] B. Vialay, D. Perraud, G. Pepin. Cahier des charges relatif à la réalisation de calculs de transport de radionucléides avec le code castem 2000. Rapport Andra, March 2001. See also Amel Sboui's thesis in <www.ann.jussieu.fr/pironneau/sboui.pdf>.

[18] J. Wagner, Finite element methods with patches and applications, Thesis 3478, EPFL, Lausanne 2006.